TÜBİTAK

Turk J Elec Eng & Comp Sci, Vol.18, No.5, 2010, © TÜBİTAK
doi:10.3906/elk-0906-55

Experimental investigation of shaft transducerless speed and position control of ac induction and interior permanent magnet motors

Ömer GÖKSU[1], **Ahmet M. HAVA**[2]
[1]*Aselsan Inc. Defense Systems Technologies, Systems Engineering, SST–SMM, 06172, Yenimahalle, Ankara-TURKEY e-mail: ogoksu@aselsan.com.tr*
[2]*Electrical and Electronics Engineering Department*
Middle East Technical University, İnönü Bulvarı, Balgat, 06531, Ankara-TURKEY
e-mail: hava@metu.edu.tr

Abstract

In order to drive AC motors with high efficiency and high motion performance, and to provide accurate speed/position control, motor shaft speed and/or position feedback is required. For this purpose, usually transducers (encoder, tachogenerator, resolver, etc.) are installed on the shaft. However, transducers are not preferred in most of the applications since they increase the cost and decrease the reliability of the drive due to their failure prone structure and connections. In such applications, the speed and/or position information of the motor is obtained by estimation methods without using shaft transducers. In this work, motor types and speed/position estimation methods will be surveyed, appropriate estimation methods will be determined based on the motor type (induction or interior permanent magnet synchronous) and the application requirement (speed and/or position control requirement). High frequency signal injection, speed adaptive flux observer, open loop integration based flux observer methods, and combination of them in a hybrid algorithm will be investigated. By implementing these methods, the experimental performance of the shaft transducerless speed and/or position controlled vector control based induction and interior permanent magnet synchronous motors will be presented. The study helps the motion control engineers select the suitable motor and implement the appropriate speed/position estimation algorithm for a given application.

Key Words: *IPM Motor, induction motor, sensorless, vector control, speed and position control, high frequency signal injection, flux observer, inverter, saliency, adaptive control*

1. Introduction

More than 65% of the electrical energy consumed in industry is utilized in three-phase AC (induction and synchronous) electrical motors [1]. Since both the energy efficiency and motion control performance are improved

substantially by supplying the motors via the adjustable speed drives (ASDs) instead of direct power line operation, ASDs are widely used in industry. Also, depending on the requirement of the application, speed and/or position control of AC motors can be provided when ASDs are employed. Since speed and position feedback are required for speed and position control, sensors (encoder, resolver, tachometer, etc.) are mounted on the motor shaft. The sensors on the motor shaft provide precise feedback for the speed and position control. However, they increase the drive system cost. Especially in low power applications, sensor cost may exceed the motor/drive cost. Precise and robust assembly of the sensor on the motor shaft requires intensive mechanical labor and the sensor can be damaged or may breakdown in harsh industrial environments. Additionally, extra hardware (cables, connectors, interface circuitry, etc.) is required for the integration of the sensors with the drives and for capturing the signals of the sensors, which result in increase of the cost, labor and failure rate. As a result, the shaft sensors increase the cost and complexity of the drive system, and decrease of the reliability due to the risk of sensor failures. For these reasons, speed/position estimation algorithms have been developed in order to provide speed/position control of the AC motors without using shaft sensors, and these algorithms are widely employed in modern ASDs [2]. Most general purpose ASD commercial products have at least one such algorithm in which the user may be able to use for the application. Estimation methods obtain the speed/position information of the motors based on the mathematical models and/or physical properties of the AC motors and using the motor current and voltage values, which are measured (for control and protection purposes) within the drive (the inverter and its microcontroller/DSP). Using the estimated speed/position information as feedback, shaft transducerless speed/position control of the motor is provided. Block diagram of a shaft transducerless drive system is shown in Figure 1. In such a drive, only the motor electrical power terminals are connected to the drive and no additional sensor feedback is necessary. Thus, compact, simple, and economical drive system is obtained.

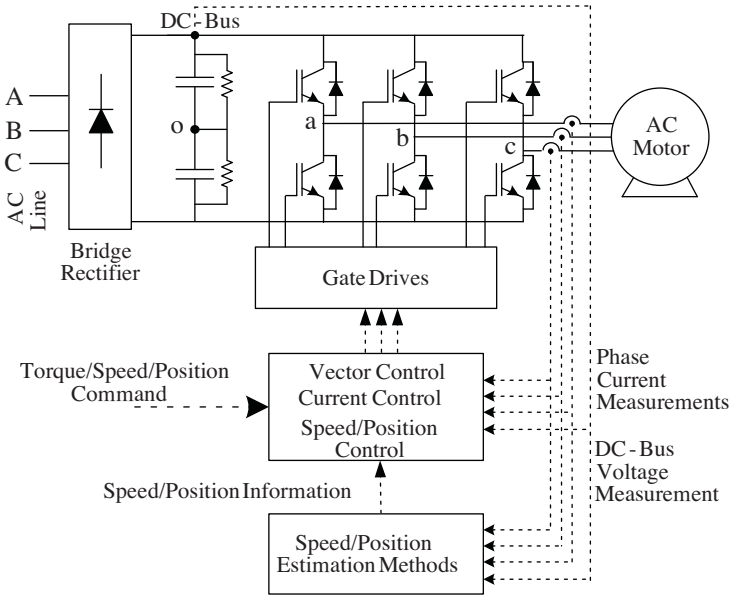

Figure 1. Shaft transducerless AC motor drive structure with speed/position estimation.

Methods based on the fundamental mathematical model of the AC motor, estimate the motor flux and speed depending on the motor back EMF using the motor parameters, the voltage applied by the inverter drive,

and the current values measured within the inverter drive [2]. Such methods do not perform satisfactorily at low and zero speed since the motor EMF is weak and its value is dominated by the inverter switch voltage drops, motor stator winding resistor voltage drops, and other disturbances. Thus, practically the EMF is not detectable (does not exist) at low and zero speed [3–5]. Also, adaptive estimation methods based on the fundamental mathematical model [6] and advanced estimation methods such as Kalman filter [7–9] and artificial neural networks are inadequate and cannot be used at low speed and especially at zero speed and zero excitation (stator) frequency cases [10]. In some applications, which do not require zero speed/frequency, such methods can be used for medium and high speed region. For instance, a shaft transducerless drive, with a rated speed of 1500 min^{-1}, does not perform well under approximately 100 min^{-1}. Nevertheless, in a wide speed range above this speed, transducerless vector control can be realized while providing high performance flux and speed/position estimation with flux observers based on the mathematical model. These methods are applied in modern commercial AC motor drives for speed control of the induction motor [2, 11], and speed/position control of interior permanent magnet synchronous motor [12, 13]. Although, the control bandwidth of the transducerless drive is decreased substantially when compared to the drive with transducer due to the delay in the estimation methods, transducerless methods are widely used in most of the modern drives since the bandwidth is adequate for most of the applications.

For speed/position estimation at the low and zero speed (zero excitation frequency) operating region, the high frequency signal injection (HFSI) method, which is based on the magnetic saliency of the AC motors, has been developed [3–5, 11, 13, 14–16]. In this approach, high frequency ($>$ 500 Hz) and low magnitude signals are imposed on the fundamental frequency main excitation signals that are associated with the power transfer of the AC motor and magnetic saliency is detected and tracked via analyzing the response of the motor at the imposed high frequency. The rotor field angle is estimated by tracking the magnetic saliency and using this angle information, speed/position control is provided. Although the induction motor does not possess magnetic saliency, magnetic saturation occurs on the excitation axis when excited with high frequency. As a result, the saturation results in impedance difference between the flux axis (d axis) and torque axis (q axis). This is termed as the artificial magnetic saliency (or induced saliency) [11]. The rotor field angle is estimated by tracking the artificial magnetic saliency. However, for the induction motor (especially for the standard closed slot type), the magnetic saturation axis deviates from the rotor field axis due to loading and the estimation accuracy decreases [11]. Therefore, HFSI, which is a method based on the magnetic saliency, can not be applied to the induction motor in general purpose commercial drives for the purpose of speed/position control at low speed. The interior permanent magnet (IPM) synchronous motor, which has recently been finding wide range of applications due to is high energy efficiency, possesses inherent magnetic saliency and its magnetic saliency can be detected and tracked with the HFSI method. As a result, in the IPM motor, shaft transducerless vector control and speed and position control is provided with high performance [13]. Based on this distinction, motor and estimator/controller types can be matched as follows. For applications which do not require operation in the zero speed (zero excitation frequency) region and/or do not require position control, the induction motor is the best choice. For such applications, methods such as the speed adaptive flux observer (SAFO) [17], perform satisfactorily and have already been in practical use for more than a decade. For applications which require high dynamic motion performance and shaft transducerless speed/position control, the IPM synchronous motor should be preferred. In the IPM motor drive, as already suggested, the HFSI method provides highly effective

solution for transducerless speed/position control and has become the trend in the recent years [5, 15, 16].

In this work, three-phase AC machine speed/position estimation methods will be surveyed, reviewed, and speed/position estimation/control performance of the motor drive systems will be experimentally verified via closing the speed/position control loops. For the induction motor, the SAFO method [17] will be investigated and shaft transducerless speed control at medium and high speed range ($\omega_r > 100$ min^{-1}) will be realized. Here, 1500 min^{-1} is assumed as base speed (high speed) for a typical industrial motor drive (employing 4-pole AC motor) and low speed corresponds to $\omega_r < 100$ min^{-1} while the range in between is assumed as medium speed. For the IPM synchronous motor, speed and position control in the medium and high speed range ($\omega_r > 150$ min^{-1}) will be provided with the integration based flux observer [12], which is based on the fundamental mathematical model. For the zero and low speed operating region ($\omega_r < 150$ min^{-1}), shaft transducerless speed and position control will be provided by employing the HFSI method [13], which is based on magnetic saliency detection and tracking. Also, combining the two methods (HFSI in the low speed range and flux observer above this range) in the same drive, a hybrid estimation/control algorithm covering the whole speed region will be created, and smooth (seamless) transition between the two methods will be provided based on the estimated speed feedback [18]. In all the estimation and control methods, rotor field oriented vector control (indirect field oriented vector control for the induction motor and direct field oriented vector control for the IPM synchronous motor) will be employed. Vector control will be provided by linear PI (proportional integral) current regulator at the synchronous frame [18, 19]. Speed control is implemented with IP (PDFF) controller, which provides high load disturbance rejection, in order to obtain high performance under the step loading condition [20–22]. In the position control loop, only proportional controller is employed.

The overall contribution of this paper involves a basic survey (mostly covering the methods which have found application in commercial drives), thorough review of selected methods, and detailed experimental investigation of sensorless control methods for AC motor drives. The paper aims to help the motion control engineer select a suitable motor and apply an appropriate sensorless control algorithm for high drive performance. Remainder of this paper is organized as follows. First, the AC induction and IPM synchronous motors will be briefly reviewed. Then, the induction and IPM synchronous machine speed/position estimation and control methods will be investigated by means of theory, simulations, and laboratory experiments. Then based on the results, conclusions and recommendations are provided.

2. Three-phase AC motors

The three-phase AC induction motor, being inexpensive and robust and easily driven, is widely used in industrial applications (air conditioner, pump, lift, etc.) for speed control via inverter drives. However, the efficiency is low since associated with it are copper and iron losses that come from drawing magnetizing current and having rotor currents due to the slip. Also, the torque performance and hence the speed control performance is inadequate for servo applications. The torque per ampere is inferior to that of a typical permanent magnet servo motor and the inertia is high. Since the torque and speed/position control performance of the permanent magnet (PM) synchronous motor is also superior, the PM synchronous motor is widely used in industry for servo applications. In the permanent magnet synchronous motor, no magnetizing current is drawn since the rotor field is created by the permanent magnets. Neither is there any rotor current and associated power losses. Thus, its efficiency

is high compared to the induction motor. The permanent magnet synchronous motor has two types depending on the installation of the permanent magnets on the rotor, as shown in Figure 2; surface mount permanent magnet (SMPM) and interior mount permanent magnet (IPM) synchronous motor. Drawings of two IPM motors showing the embedded magnets are shown in Figure 3.

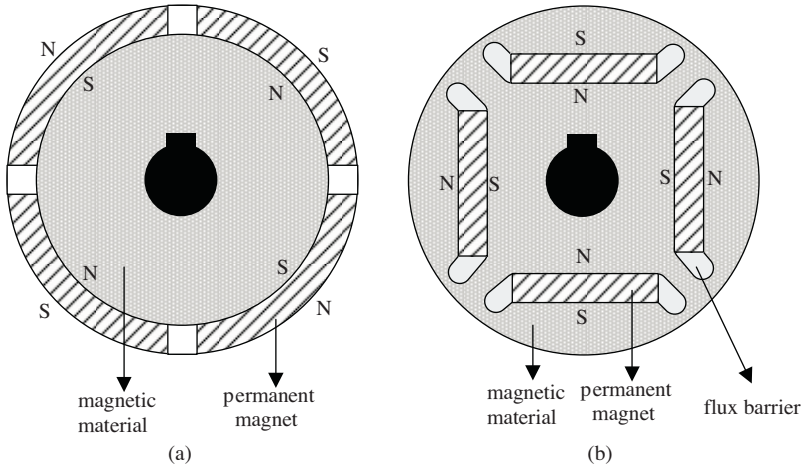

Figure 2. Surface mount permanent magnet (SMPM) rotor (a) and interior permanent magnet rotor (b) structures.

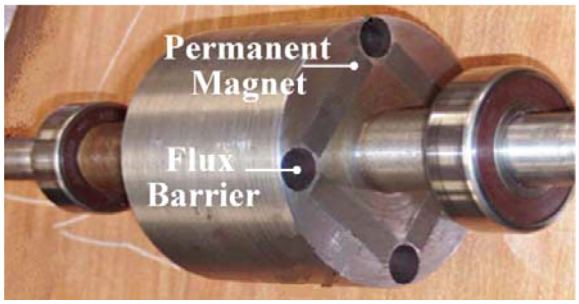

Figure 3. The interior mount permanent magnet (IPM) rotor structure with embedded magnets.

Since the flux distribution is enhanced in the IPM synchronous motor due to the embedded magnets, more dense and sinusoidal shaped flux can be created. The torque and power density of the motor increases, efficiency improves, and torque ripple decreases. Since the magnets are embedded, the air-gap between the rotor and stator is small, and hence the synchronous inductance values can be kept high. Thus, voltage can be created against the EMF via the voltage on the reactance, and the motor can be driven to high speeds by field weakening. The field weakening method is not effective for the SMPM synchronous motor since the inductance values are low. Since many industrial applications require high speed operating capability, the field weakening property of the IPM synchronous motor makes it a strong competitor of the induction machine.

In the IPM motor, the reluctance is high and inductance is low on the d-axis (flux axis), where the magnets lay. The reluctance is low and inductance is high on the q-axis, which is in quadrature to the d-axis. Hence, there exists significant reluctance difference between the d-axis and the q-axis, and the IPM motor possesses inherent magnetic saliency property. This property enables the sensorless speed/position control of the IPM motor with the HFSI method, which is based on the magnetic saliency, at low and zero speed. Based

on the flux and currents defined in an synchronous frame, the saliency creates the reluctance torque of an IPM motor can be expressed as

$$T_e = \frac{3}{2}\frac{p}{2}\left[\underbrace{\lambda_f I^e_{qs}}_{\text{synchronous torque}} + \underbrace{(L^e_{ds} - L^e_{qs})I^e_{ds}I^e_{qs}}_{\text{reluctance torque}}\right], \quad (1)$$

where p is the pole number, λ_f is the rotor magnetic field (flux linkage), L^e_{ds} and L^e_{qs} are the inductances on the d and q axis, i^e_{qs} is the torque current, and i^e_{ds} is the flux producing current. Since L^e_{ds} is smaller than L^e_{qs} in the IPM motor, negative i^e_{ds} flux producing current provides both field weakening and the reluctance torque. When the magnetic saliency ratio (L^e_{ds}/L^e_{qs}) of the IPM motor is high, the torque density of the motor can be optimized by selecting the d and q axis currents such that maximum torque per ampere is obtained [23].

In summary, the induction motor has been widely used in speed control requiring industrial applications, while the SMPM synchronous motor has been widely used in servo applications with its superior speed and position control performance. Pioneered in 1980's, and its technology matured through the 1990's, the IPM synchronous motor is increasingly finding applications in industrial drive and servo applications [24, 25]. Its use in industrial (e.g., air conditioner, pump, lift, etc.) and domestic (e.g. air conditioner) applications has been widely accepted due to its high efficiency. For instance, since 2003, the IPM motor has replaced all induction motors in air conditioner systems in Japan, where energy efficiency is critical. In typical air conditioning systems, the efficiency is 73% in the induction motor, where it is 86% in IPM motor [24, 25]. Not only the energy efficiency, but also the sensorless speed/position control capability of this motor, has made it a strong competitor to the induction motor. In many applications only the IPM synchronous motor drive system meets the reliability, performance, and cost criteria. Thus, its application is rapidly spreading.

3. Sensorless speed control of the induction motor

Sensorless speed control of the induction motor is realized with the SAFO [17] method, which is based on the fundamental mathematical model (standard induction motor equivalent circuit). The rotor flux angle is obtained by using the estimated motor speed information, and indirect field oriented control is provided. Also, the estimated speed information is used as feedback for the precise speed control of the motor.

3.1. Estimation of the rotor flux and shaft speed of the induction motor with the speed adaptive flux observer (SAFO)

SAFO [17] is an adaptive state observer, which is based on the fundamental mathematical model of the induction motor. The unmeasured state variables, which are the rotor flux and shaft speed, are estimated with SAFO. The SAFO structure is given in Figure 4. It uses the known/measured/estimated motor parameters (equivalent circuit resistance and inductance values) and the stator current and voltage values, which are measured within the drive.

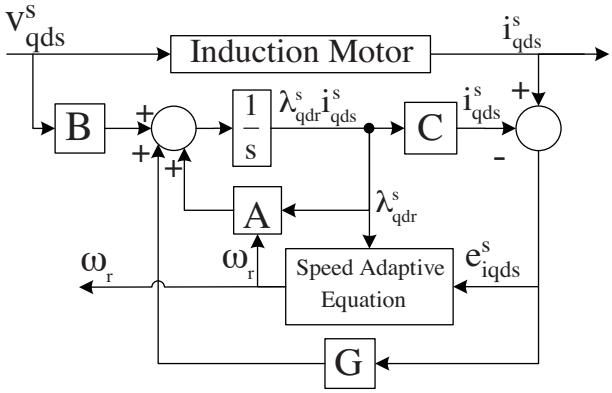

Figure 4. The structure of the speed adaptive flux observer (SAFO).

The state space equation of the SAFO method, which is based on the state observer theory and defined in stationary (ds-qs) vector coordinates, is given by

$$\frac{d}{dt}\begin{bmatrix} \hat{\lambda}^s_{qdr} \\ \hat{i}^s_{qdr} \end{bmatrix} = \hat{A}\begin{bmatrix} \hat{\lambda}^s_{qdr} \\ \hat{i}^s_{qdr} \end{bmatrix} + B\left[v^s_{qds}\right] + G\left[i^s_{qds} - \hat{i}^s_{qds}\right]. \tag{2}$$

Here, $\hat{A}$, B, and G are model state, input, and observer gain matrices, respectively; and v^s_{qds}, i^s_{qds} and $\hat{\lambda}^s_{qdr}$ are the stator voltage, current, and estimated flux vectors. The state matrix involves the motor parameters (resistance and inductance values) and the estimated speed. The error equations of the observer are given by

$$e = \left[i^s_{qds} - \hat{i}^s_{qds}\right], \tag{3}$$

$$\frac{d}{dt}e = (A - GC)e - \Delta A\begin{bmatrix} \hat{\lambda}^s_{qdr} \\ \hat{i}^s_{qdr} \end{bmatrix}. \tag{4}$$

The main error component in the state matrix is the estimated speed variable. The Lyapunov stability of the observer is investigated with the Lyapunov equation [17]

$$V = e^T e + (\hat{\omega}_r - \omega_r)^2/F \tag{5}$$

Here, $\hat{\omega}_r$ represents the estimated speed, ω_r the actual speed, and F a positive constant. When the motor speed is estimated with the adaptive equation (6) in the SAFO structure, the SAFO possesses Lyapunov stability:

$$\hat{\omega}_r = K_p(e_{ids}\hat{\lambda}^s_{qr} - e_{iqs}\hat{\lambda}^s_{dr}) + K_I\int(e_{ids}\hat{\lambda}^s_{qr} - e_{iqs}\hat{\lambda}^s_{dr})dt \quad . \tag{6}$$

In the SAFO method, using the error between the estimated and measured stator currents, and the estimated flux values in the speed adaptive equation (6), and selecting the K_P, K_I parameters appropriately, the estimated motor speed converges to the actual motor speed. Estimated by the adaptive equation, the speed value is used in the state matrix $\hat{A}$ in the state observer, in vector control for obtaining the rotor flux angle, and in speed control

as speed feedback. High performance speed control is provided by designing the vector control based current regulator in synchronous (de-qe) coordinates and the motor speed controller with high bandwidth. Here, motor parameters are assumed to be constant. In practice, they can change during operation steady-state estimation error may occur. However, online parameter estimation methods can improve the estimation accuracy and stability [10].

3.2. The experimental results of the induction motor speed control

A Texas Instruments TMS320F2808 DSP control platform-based AC drive and a motor test bench are developed in the laboratory in order to implement the speed control of the induction motor with the SAFO method. A 3.6 kW SMPM synchronous motor (Kollmorgen-AKM54N) is used as load for the 4-kW 4-pole induction motor (Siemens-1LA7-113-4AA), whose speed is sensorless controlled. The induction motor is driven in speed control mode based on indirect field oriented vector control by using the speed information estimated by the SAFO method. The DC bus voltage of the inverter drive is 500 V and the PWM frequency is 5 kHz. The current regulator and estimation algorithms are updated at 10 kHz by sampling the phase currents twice for each PWM period (double update). An incremental encoder (Thalheim-ITD20A4-1024) is mounted on the induction motor shaft in order to monitor the estimation accuracy. The block diagram and the photograph of the experimental setup are given in Figure 5 and Figure 6. The parameters used [18] for the current regulator, speed adaptive equation, and speed controller within the SAFO method are given in Table I.

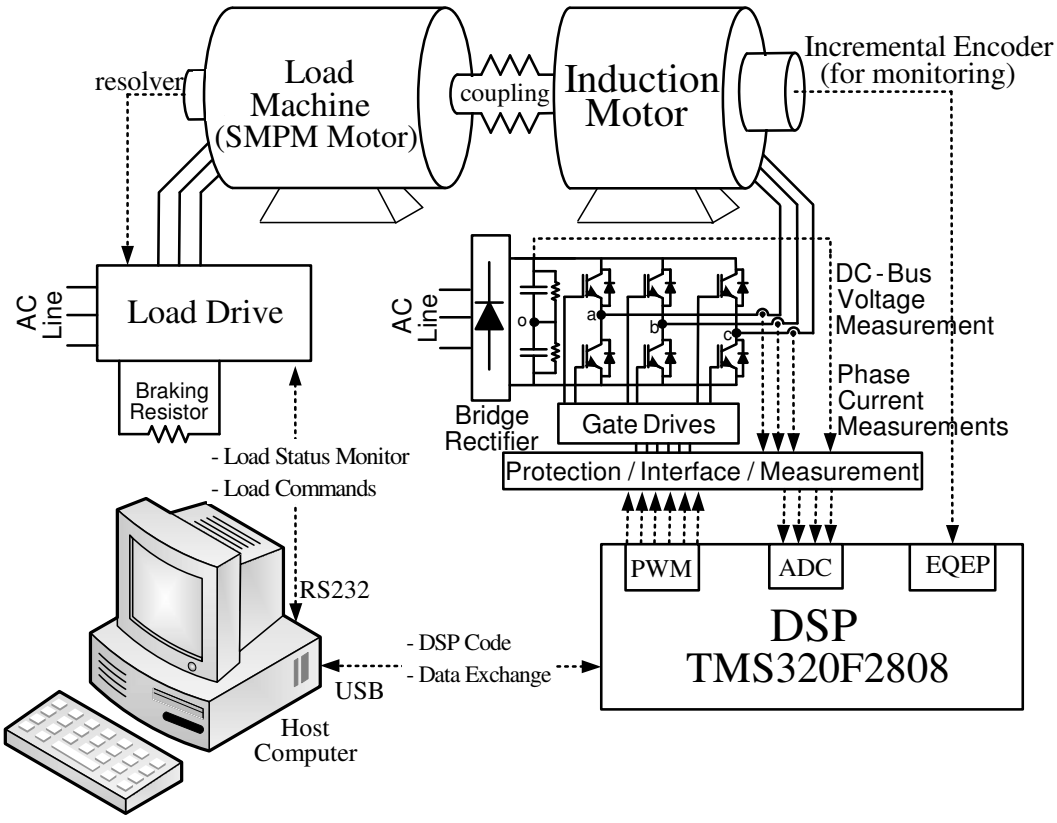

Figure 5. Experimental setup block diagram.

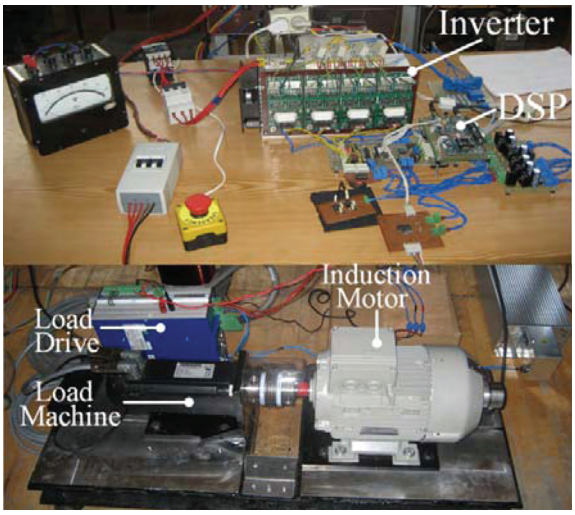

Figure 6. Induction motor experiment setup.

Table 1. Parameters used within the speed adaptive flux observer experiments.

Synchronous Frame Current Regulator	K_p	100
	K_I	16400
	LPF on the feedback path	2^{nd} order with 1 kHz cut-off
Speed Adaptive Scheme Gains	K_P of the compensator	0.5
	K_I of the compensator	100
Speed Controller	K_{pr}	1
	K_p	0.072
	K_I	2

In Figure 7, the sensorless speed control of the induction motor is realized with the speed estimated by the SAFO method. The estimation accuracy is high at 600 min^{-1} constant speed. When a 15 Nm step load (50% of the induction motor rated torque) is applied to the motor shaft with the load machine and removed, the estimated speed tracks the actual speed accurately and speed control based on the estimated speed is realized with high performance under loading conditions. In Figure 8, the speed command is increased from 100 min^{-1} to 500 min^{-1}, when the induction motor is under 7.5 Nm (25% of the induction motor rated torque) load. The SAFO estimated speed tracks the actual speed accurately and speed control based on the estimated speed is realized with high performance under loading conditions. Sensorless control is provided with stability and high dynamic performance, down to 7% of the rated speed. Below this speed, the performance of the sensorless drive degrades significantly and operating in this range is not recommended, as this is the case in most commercial drives with sensorless control.

4. IPM motor speed / position control

For the sensorless control of the IPM motor; the magnetic saliency based HFSI method at low and zero speed, and the integration based flux observer at high speed, are employed. Moreover, these two methods are combined in a single algorithm, the method is selected based on the estimated speed, and smooth motion is provided by

providing smooth (seamless) transition between the two methods. Hence, high performance speed and position estimation and control are provided for the whole speed range with a single algorithm (unlike the induction motor drive which is difficult to operate sensorless near zero speed).

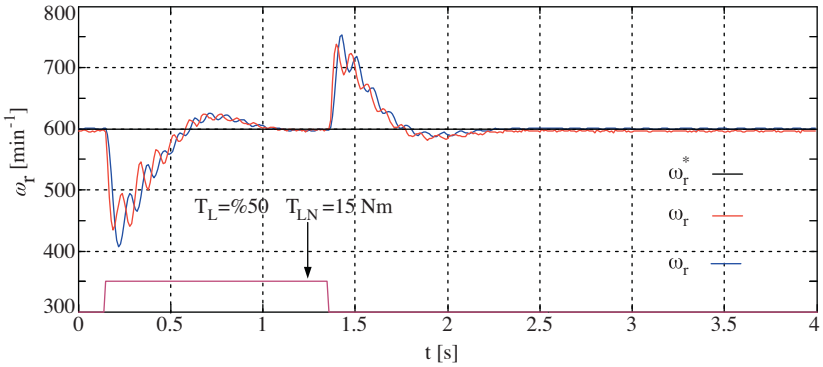

Figure 7. The commanded speed (black), actual speed (red), estimated speed (blue) and the load (purple) for 50% step load at constant speed with SAFO method.

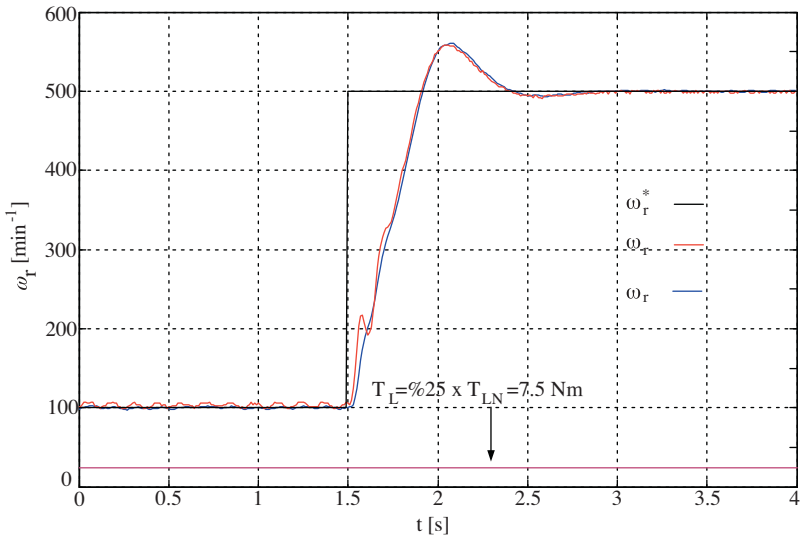

Figure 8. The commanded speed (black), actual speed (red), estimated speed (blue) and the load (purple) for acceleration under 25% constant load with SAFO method.

4.1. High frequency signal injection (HFSI) method

The IPM motor has the magnetic saliency property due to the installation of the magnets. The elliptic current and admittance characteristics in Figure 9 are obtained when the stator windings are excited with high frequency voltage vectors at various angles while the rotor is locked. Lowest impedance and highest current are observed on the magnet axis (de-axis) of the rotor. In Figure 10, the admittance curve of the stator windings with respect to the flux (magnet) axis of the rotor is shown.

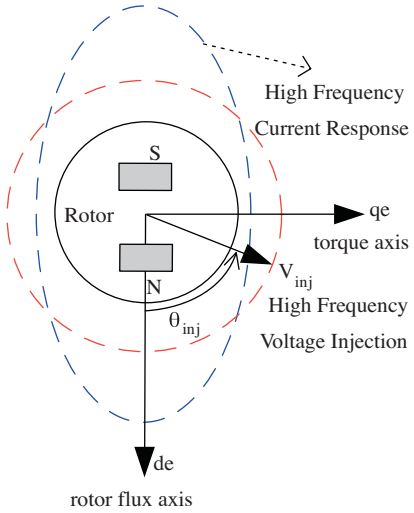

Figure 9. The saliency characteristic of the IPM motor.

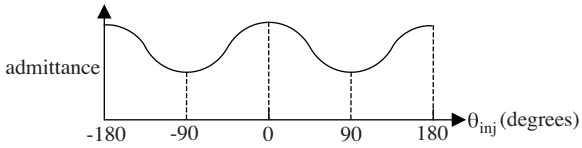

Figure 10. The admittance curve of the IPM motor (w.r.t. rotor flux angle).

In the HFSI method, the rotor magnet axis is estimated by detecting and tracking the highest admittance value via exciting the stator windings with high frequency voltage or current vector, which is superposed on the fundamental frequency excitation. Vector control and speed/position control is provided by using the estimated magnet axis angle information. Since the admittance ellipse of the IPM motor rotates with the rotor and exists even at zero speed, the magnetic saliency based HFSI method is successful at zero and low speed. Thus, it is practically applicable in applications requiring sensorless position/speed control at low and zero speed. In the HFSI method, since the high frequency signal has low magnitude and high frequency, it does not disturb the fundamental frequency operation of the motor; however, small amount of torque ripple due to the reluctance torque and audible noise may occur. The high frequency signal can be voltage or current and can be applied as pulsating or rotating at stationary or synchronous coordinates. In this work, pulsating voltage signal (vector) is applied to the estimated rotor axis (magnet axis) for high frequency excitation [11], [13]. The applied voltage and current waveforms of this method are shown in Figure 11 with the PWM ripples removed from the waveforms. These simulated waveforms are obtained with an injection signal frequency of 250 Hz (for visual clearance the injection signal frequency is selected quite low compared to practical injection frequencies).

The block diagram of the IPM drive system, where the HFSI method applied, is given in Figure 12. The vector control at the fundamental frequency is implemented based on the estimated rotor flux angle information. High frequency low magnitude voltage is added to the fundamental frequency voltage. The fundamental frequency operation is provided by low-pass-filtering the high frequency signals from the motor phase currents in the DSP. The high frequency current information is obtained by band-pass-filters. The maximum admittance angle is tracked with a structure similar to a phase-lock-loop (PLL) [18]. Hence, rotor flux angle is estimated. The mechanical speed/position information is obtained from the estimated angle

information and speed/position control of the IPM motor based on vector control is provided.

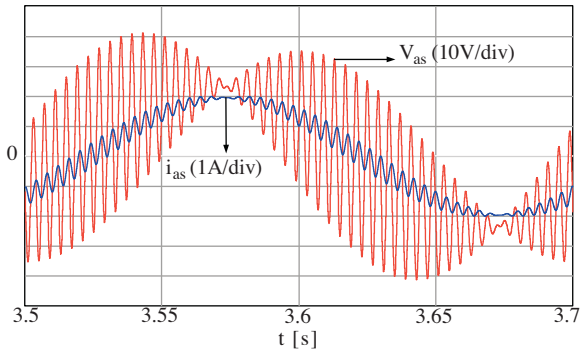

Figure 11. The applied phase voltage (red) and induced current (blue) waveforms when the HFSI method is used (10 Hz fundamental, 30 V / 250 Hz high frequency signals).

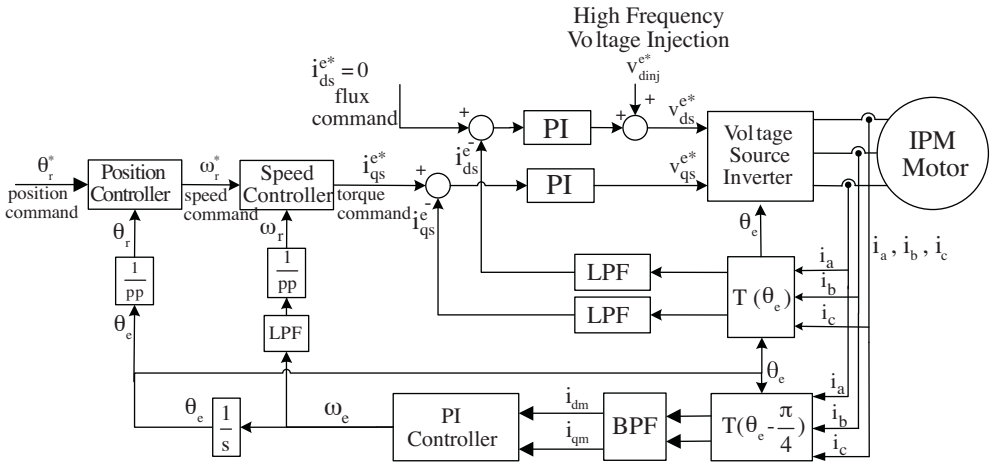

Figure 12. The block diagram of the IPM motor drive system with sensorless vector control based on the HFSI method.

4.2. The experimental results for the IPM motor with HFSI method

For experimental implementation of sensorless speed/position controlled system, a 2.2 kW, 6 poles, 368 V, 1450 $\min^{-1}$ (L_d=46.42 mH, L_q=60.32 mH, R_s=2.656 Ω) IPM motor (Yaskawa Varispeed-686SS) motor is used. The experimental test-bench, which involves the IPM motor and the servo drive providing loading is shown in Figure 13. The discussed estimation methods and the sensorless vector control algorithm is implemented on the DSP based inverter of Section 3.2. In the experiments, an HFSI injection voltage with 75 V magnitude and 500 Hz frequency is applied and sensorless speed/position estimation and motion performances are investigated. Since the magnetic saliency ratio of the IPM motor, which is used in this work, is not so high (0.456) [18]; the maximum torque per amper optimization or field weakening are not applied, thus the flux current reference value (i^e_{ds}) is set to zero value. The parameters used [18] in the current regulator, HFSI algorithm, speed controller, and position controller of the system are given in Table II.

Figure 13. IPM motor experimental setup.

Table 2. Parameters used within the high frequency signal injection experiments.

Synchronous Frame Current Regulator	K_p	7.5
	K_I	930
	LPF on the feedback path	2^{nd} order with 100 Hz cut-off
High Frequency Signal Injection Algorithm	BPF	4^{th} order wide band-pass with 100 Hz low cut-off and 2500 Hz high cut-off
	LPF within the heterodyning	2^{nd} order with 20 Hz cut-off
	K_P of the compensator	2000
	K_I of the compensator	100
Speed Controller	K_{pr}	0.5
	K_p	0.012
	K_I	0.2
Position Controller	K_p	20

The trapezoidal speed profile command response of the speed controlled IPM motor, whose speed and position are estimated with the HFSI method, is shown in Figure 14. The response to acceleration command from 0 min^{-1} to 150 min^{-1}, when the IPM motor is under constant 15 Nm (100% of rated torque) load, is shown in Figure 15. It is observed from these experiments that the estimated speed tracks the actual speed. The rotor flux angle is estimated with high accuracy and the speed controller realizes the commanded speed using the estimated speed information. The 7.5 Nm (50% rated torque) step load response of the IPM motor (when constant 0° position is commanded), whose speed and position are estimated with the HFSI method and the position is controlled, is shown in Figure 16. It is observed that, the position and speed estimation and hence the sensorless position control is realized with high accuracy.

The position estimation error, which is less than 5° for no-load case, increases with loading (becomes less than 20°), since the maximum admittance angle deviates from the magnet axis due to magnetic saturation with loading. The estimation error due to loading can be sufficiently compensated within drive by using the torque current information. As observed from the experiments, the IPM motor can be successfully sensorless position-controlled with the HFSI method [18]. Large oscillations are observed both in estimated speed and position partially due to current feedback measurement noise in the experimental system and partially due to high gains used in the compensator of the HFSI algorithm, where high compensator gains are needed for better estimation dynamics. These speed oscillations can be damped by the inertia of the load. However, they can be disturbing in applications with very high motion precision requirements. Another estimation error component for the HFSI algorithm is the delays introduced by the filters employed in the HFSI algorithm. In [26], an on-

line compensation method is proposed based on the group delay theory. The method determines the position estimation error compensation based upon a demodulation delay and a velocity or rotational frequency of the motor, which substantially minimizes the error.

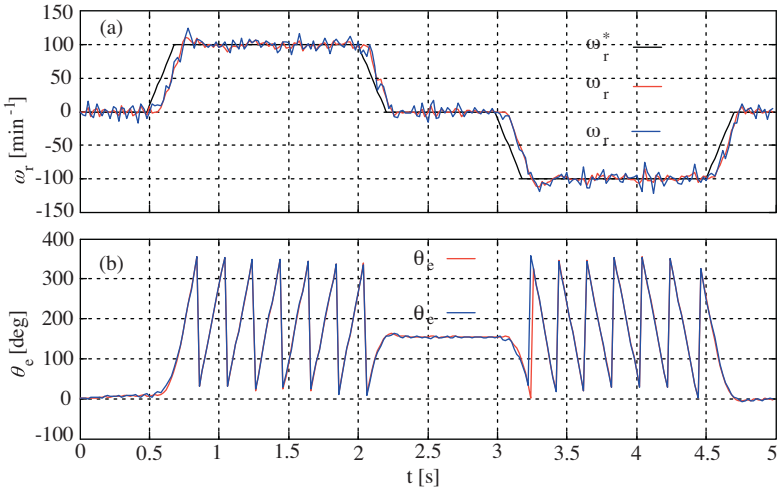

Figure 14. The commanded speed (black), actual speed (red), estimated speed (blue) (a) actual rotor angle (red) estimated rotor angle (blue) (b) for the no-load trapezoidal speed profile with HFSI method.

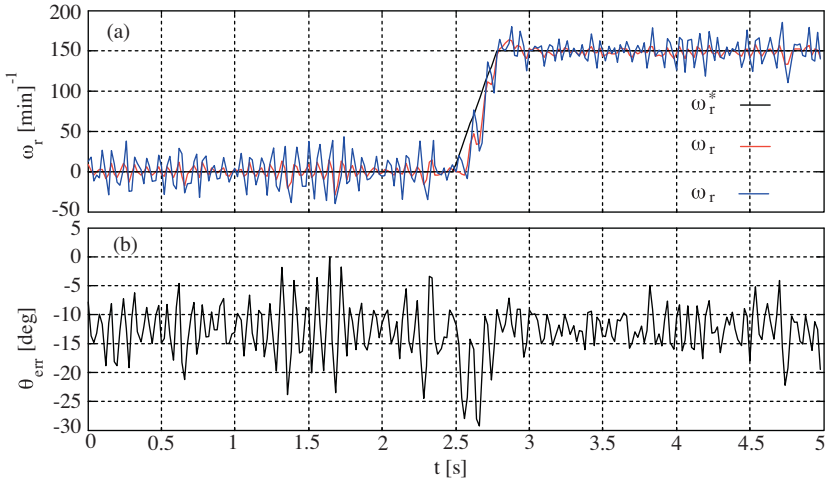

Figure 15. The commanded speed (black), actual speed (red), estimated speed (blue) (a) rotor angle estimation error (b) for acceleration under constant (100%) load with HFSI method.

4.3. Estimation with integration based flux observer (IFO)

The sensorless speed and position control of the IPM motor at high speed is provided with the IFO method, which detects the back EMF based on the fundamental mathematical model of the IPM motor [12]. Since the speed/position control at the low and zero speed regions is provided with the HFSI method, the IFO algorithm is

not employed (it is not required) at low speed and the adaptive methods are not used to improve the performance of IFO at low speed. In the IFO method, the stator flux is estimated by solving the mathematical model of the IPM motor at stationary coordinates, and the rotor flux is obtained from the estimated stator flux by calculating the load angle information. The rotor flux angle estimation is used in vector control and speed/position control. The stator flux and flux angle estimation equations are given the relations

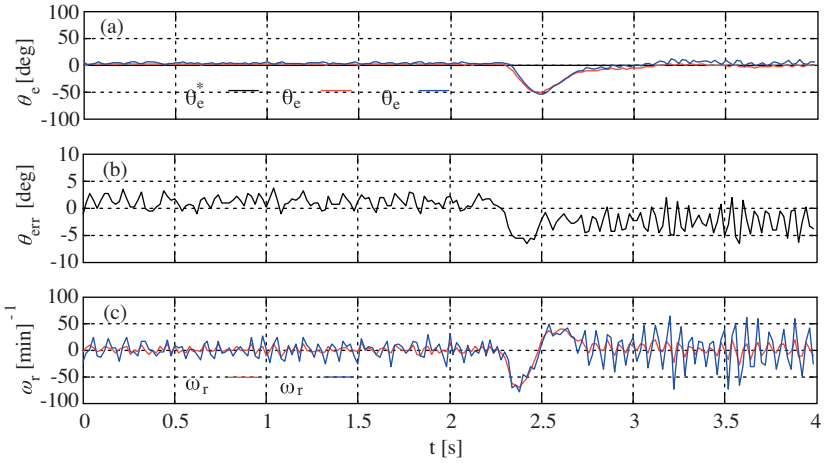

Figure 16. The commanded position (black), actual position (red), estimated position (blue) (a) rotor angle estimation error (b) actual speed (red), estimated speed (blue) (c) step (50%) load under constant 0° position command with HFSI method.

$$\hat{\lambda}^s_{qds} = \int_{t_0}^{t} (V^s_{qds} - R^i_s)dt, \tag{7}$$

$$\hat{\theta}_s = tan^{-1}(\lambda^s_{qs}/\lambda^s_{ds}) \quad ; \tag{8}$$

the load angle is given by the equation

$$\delta = tan^{-1}[L_q i^e_{qs}/(L_d i^e_{ds} + \lambda_f)]; \tag{9}$$

and the rotor flux angle estimation equation is given by

$$\hat{\theta}_e = \hat{\theta}_s - \delta. \tag{10}$$

The parameters used [18] in the current regulator, speed controller, and position controller of the IFO method are given in Table III.

4.4. The experimental results for the IPM motor with the hybrid HFSI-IFO algorithm

The speed/position control of the IPM motor with the IFO method is implemented in the experimental setup of Section 4.2. The IFO method is utilized when the motor speed is larger than 150 min^{-1}, where the motor is

brought to that speed by the HFSI method. The HFSI (up to 150 $\min^{-1}$) and IFO (above 150 $\min^{-1}$ speed) methods are combined and applied in the hybrid algorithm, which provides smooth transition based on the estimated speed and covers the whole speed range. The current/speed/position parameters are adapted (from the parameters in Table II to parameters in Table III) during the transition between two algorithms [18]. The two algorithms are employed separately in this work, however, both algorithms can be utilized at the same time as a fusion of two estimation sources, for improved response [27]. The response to acceleration from 0 $\min^{-1}$ to 750 $\min^{-1}$ under constant 7.5 Nm (50% rated torque) is shown in Figure 17. It is observed that the estimation is accurate with both methods, transition is smooth and motion performance is high.

Table 3. Parameters used in the flux observer experiments.

Synchronous Frame Current Regulator	K_p	75
	K_I	9300
	LPF on the feedback path	2^{nd} order with 1 kHz cut-off
Speed Controller	K_{pr}	0.5
	K_p	0.08
	K_I	0.01
Position Controller	K_p	20

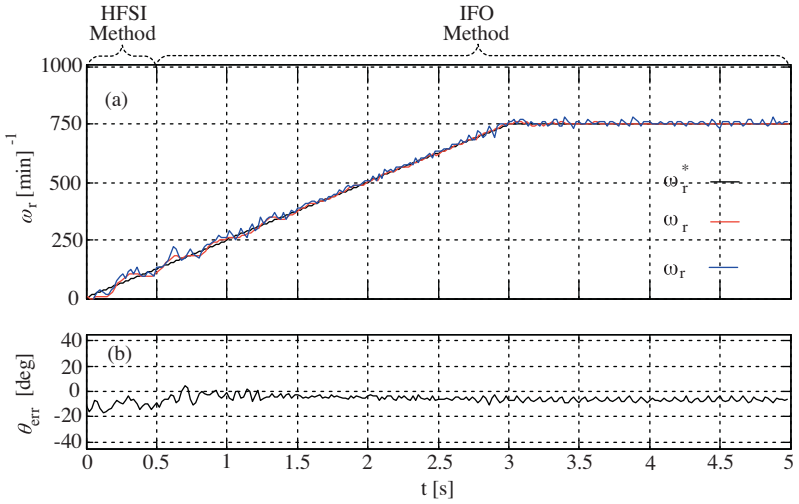

Figure 17. The commanded speed (black), actual speed (red), estimated speed (blue) (a) rotor angle estimation error (b) for acceleration under constant (50%) load with hybrid method.

5. Conclusion

In this work speed/position estimation methods developed for the purpose of speed/position control of the AC motors without using shaft transducers, are surveyed, reviewed, and experimentally investigated. It is shown that except for the zero and low speed region, the speed estimation of the induction motor with the speed adaptive flux observer method (which uses the fundamental mathematical model) provides high performance. It is accurate in a wide operating speed region and as a result, closing the speed control loop, high performance sensorless vector control and high performance speed control are achieved. Also, it is shown that the speed

and position estimation and hence the control for the IPM motor, which has strong magnetic saliency, can be realized even at low and zero speed with high performance by employing the high frequency signal injection method. The integration based flux observer is employed for the high speed solution of the IPM motor. The hybrid algorithm, which covers the whole speed range by combining the two methods, is implemented and high performance is obtained. The theory is verified with experiments.

Based on the theoretical and experimental investigations, it has been illustrated that the success of the sensorless control methods depends on the motor type. The best results can be obtained by matching a motor type with a suitable sensorless control algorithm. The matching process indicates that the induction motor and SAFO algorithm is a good match yielding a sensorless induction motor drive with a wide speed operating range (except near zero speed/stator frequency range). In the applications requiring sensorless speed/position control in a wide range including zero speed/stator frequency, the IPM motor with HFSI algorithm at low speed and EMF detection based observer at high speed forms a good match. Although the higher cost IPM motor increases the cost of the system, the additional benefit of higher efficiency favors this motor drive over the induction motor drive for the future. The thorough experimental work confirms that the good match yields satisfactory results and the typical motion control requirements are met by the suggested systems. Thus, motion control engineers can (should) select their motors and inverter drives based on the suggested method.

References

[1] A. Savolainen, "Driving towards a Better Future," *ABB Review 4/2004*, pp.34-38.

[2] J. Holtz, "State of the art of controlled AC drives without speed sensor," *IEEE-PEDS Conf. Records*, pp. 1-6, 1995.

[3] P. L. Jansen, R. D. Lorenz, "Transducerless Position and Velocity Estimation in Induction and Salient AC Machines," *IEEE Transactions on Industry Applications*, Vol. 31, No. 2, pp. 240-247, March/April 1995.

[4] J. I. Ha, S. K. Sul, "Sensorless field-orientation control of an induction machine by high-frequency signal injection," *IEEE Transactions on Industry Applications*, vol. 35, no. 1, pp. 45–51, January/February 1999.

[5] K. Ide, J. I. Ha, M. Sawamura, H. Iura, Y. Yamamoto, "A novel hybrid speed estimator of flux observer for induction motor drives," In *IEEE International. Symposium on Industrial Electronics Records*, vol. 3, pp. 822-827, L Aquila, Italy, July 2002.

[6] Y. Li, N. Ertugrul, "A Novel, Robust DSP-Based Indirect Rotor Position Estimation for Permanent Magnet AC Motors Without Rotor Saliency," *IEEE Transactions on Power Electronics*, Vol. 18, No. 2, pp. 539-546, March 2003.

[7] B. Akin, U. Orguner, A. Ersak, M. Ehsani, "Simple derivative-free nonlinear state observer for sensorless AC drives," *IEEE/ASME Transactions on. Mechatronics,* vol. 11, no. 5, pp. 634–643, October 2006.

[8] Y.R.Kim, S.K.Sul, and M.H.Park, "Speed sensorless vector control of induction motor using extended Kalman filter," *IEEE Trans. Industry Applications,* vol. 30, no.5 pp.1125-1233, October 1994.

[9] M. Barut, S. Bogosyan, and M. Gokasan, "Speed-sensorless estimation for induction motors using extended Kalman filters," *IEEE Trans. Ind. Electron.,* vol. 54, no. 1, pp. 272–280, Feb. 2007.

[10] H. Kubota, I. Sato, Y. Tamura, K. Matsuse, H. Ohta, Y. Hori, "Regenerating-mode low-speed operation of sensorless induct*ion motor drive with adaptiv*e observer," *IEEE Transactions on Industry Applications*, vol. 38, no. 4, pp. 1081-1086, July/August 2002.

[11] J.-I. Ha, S.-K. Sul, K. Ide, I. Murokita, K. Sawamura, "Physical understanding of high frequency injection method to sensorless drives of an induction machine," *IEEE-IAS Conf. Records*, Vol. 3, pp. 1802-1808, 2000.

[12] R. Wu, G. R. Slemon, "A permanent magnet motor drive without a shaft sensor," *IEE Trans. Ind. Applicat.*, vol. 27, pp. 1005-1011, May 1991.

[13] J.-I. Ha, K. Ide, T. Sawa, S. Sul, "Sensorless position control and initial position estimation of an interior permanent magnet motor," *IEEE-IAS Conf. Records*, pp. 2607-2613, 2001.

[14] P. L. Jansen, R. D. Lorenz, "Transducerless field orientation concepts employing saturation-induced saliencies in induction machines," In *IEEE-IAS Conf. Records*, pp. 174–181, Orlando, USA, 1995.

[15] Y. Jeong, R. D. Lorenz, T. M. Jahns, S. K. Sul, "Initial rotor position estimation of an interior permanent magnet synchronous machine using carrier-frequency injection methods," In *IEMDC Records*, pp. 1218-1223, June 2003.

[16] J. I. Ha, K. Ide, T. Sawa, S. K. Sul, "Sensorless rotor position estimation of an interior permanent magnet motor from initial states," *IEEE Transactions on Industry Applications*, vol. 39, no. 3, pp. 761–767, May/June 2003.

[17] H. Kubota, K. Matsuse, T. Nakano, "DSP-based speed adaptive flux observer of induction motor," *IEEE Trans. Ind. Applicat.*, vol. 29, no. 2, pp. 344-348, 1993.

[18] Ö. Göksu, "Shaft transducerless vector control of the interior permanent magnet motor with speed and position estimation using high frequency signal injection and flux observer methods," M.S. Thesis, Middle East Technical University, Ankara, 2008.

[19] F. Briz, M. W. Degner, R. D. Lorenz, "Analysis and design of current regulators using complex vectors," *IEEE Transactions on Industry Applications*, vol. 36, no. 3, pp. 817-825, May/June 2000.

[20] G. Ellis, R.D. Lorenz, "Comparison of motion control loops for industrial applications," In *IEEE-IAS Conf. Records*, vol. 4, pp. 2599 – 2605, October 1999.

[21] D. Y. Ohm, "Analysis of PID and PDF compensators for motion control systems," In *IEEE-IAS Conf. Records*, vol. 3 pp. 1923-1929, October 1994.

[22] G. Ellis, "Control System Design Guide," Academic Press, 2000.

[23] Jang-Mok Kim, Seung-Ki Sul, "Speed control of interior permanent magnet synchronous motor drive for the flux weakening operation," *IEEE Transactions on Industry Applications*, vol.33, pp. 43-48, 1997.

[24] M. A. Rahman, "Recent advances of IPM motor drives in power electronics world," *IEEE-PEDS Conf. Records*, pp. 24-31, 2005.

[25] M.J. Melfi, S.D. Rogers, S. Evon, B. Martin, "Permanent-magnet motors for energy savings in industrial applications," *IEEE Transactions on Industry Applications*, vol.45, pp. 1360-1366, 2008.

[26] J. Liu, T. Nondahl, P. Schmidt, S. Royak and M. Harbaugh, "An On-line Position Error Compensation Method for Sensorless IPM Motor Drives Using High Frequency Injection," In *IEEE-ECCE 2009 Conference Records*, pp. 1946-1953, San Jose, California, USA, September 2009.

[27] M. Hinkkanen, V.M. Leppanen, J. Luomi, " Flux Observer Enhanced With Low-Frequency Signal Injection Allowing Sensorless Zero-Frequency Operation of Induction Motors," *IEEE Transactions on Industry Applications*, vol.41, no.1, pp. 52-59, 2005.